

Effects of Metallic Glass Precursors on the Catalytic Performance of Nanoporous Metals

Sheng-chen Yang^a, Mei-ping He^a, Yu-Qiao Zeng^{a*}, Xuhai Zhang^a, Jianqing Jiang^a, Akihisa Inoue^b

^aJiangsu Key Laboratory of Advanced Metallic Materials, School of Materials Science and Engineering, Southeast University, Nanjing, 211189, China

^bInstitute for Materials Research, Tohoku University, Sendai, 980-8577, Japan

Received: September 30, 2014; Revised: September 5, 2015

This work reports the effects of metallic glass precursors on the catalytic performance of nanoporous metals. Pd-based multicomponent nanoporous metals with similar nanoporous structure were successfully fabricated by electrochemically dealloying the Pd₂₀Ni₆₀P₁₇B₃ and Pd₂₀Ni₂₀Cu₄₀P₁₇B₃ metallic glass precursors at the critical dealloying potentials. It was found that the glassy precursors with different chemical compositions result in different doping elements in the as-obtained nanoporous metals and thus lead to different catalytic activities.

Keywords: metallic glass, nanoporous metal, dealloying, catalysis, formic acid

1. Introduction

When compared with the other batteries, fuel cells have a great advantage in energy storage and conversion¹. However, the high cost and low durability of Pt-based catalysts pose a severe challenge to the commercialization of fuel cells. Pd catalysts are one of the most promising candidates for the Pt-based catalysts since they have lower cost and exhibit less toxicity for formic acid oxidation². Moreover, the Pd-based catalysts show high catalytic activities towards the oxidation of the formic acid when they are combined with transition metals³. However, it is difficult to dope multiple elements in the catalysts and most of the reported Pd-based catalysts are binary. In this study, we will report the formation of multicomponent Pd-based nanoporous catalysts by dealloying metallic glasses and the effects of the glassy precursor compositions on the catalytic performance of the as-obtained nanoporous catalysts will be discussed. Dealloying is a simple and effective way to fabricate nanoporous metals (NPMs) with well-defined structures, which have functional applications in a wide field such as catalysis and chemical sensors⁴⁻⁹. Usually, a monolithic phase should be used as the dealloying precursor to form a uniform nanoporous structure since the nanopores are formed by a self-assembly process instead of excavating one phase from a pre-separated multiphase system¹⁰⁻¹². So far, only limited solid solutions and intermetallic alloys have been proved as ideal precursors. Recently, there are some attempts to synthesize NPMs by dealloying amorphous materials. Among these amorphous materials, the metallic glasses are one of the most conspicuous systems which have a homogeneous composition and structure down to subnanoscale. Till now, more than thousands of metallic glass systems have been developed and most of them contain more than three kinds of elements. Chen et al.¹³ pioneered synthesizing NPMs through electrochemically dealloying metallic glasses. Using the Pd₃₀Ni₃₀P₂₀ glass as a precursor, they successfully prepared pure NPPd. Following

the landmark work of Chen, several NPMs such as NPCu and NPTi were synthesized by dealloying metallic glasses. In this work, we use the Pd₂₀Ni₆₀P₁₇B₃ and Pd₂₀Ni₂₀Cu₄₀P₁₇B₃ metallic glassy ribbons to form Pd-based NPMs with Ni, Cu and P elements.

2. Experiment Methods

The Pd₂₀Ni₆₀P₁₇B₃ and Pd₂₀Ni₂₀Cu₄₀P₁₇B₃ metallic glassy ribbons were produced by single-roller melt spinning. The amorphous structure was confirmed by X-ray diffraction (XRD). The polarization tests and the dealloying of the Pd₂₀Ni₆₀P₁₇B₃ and Pd₂₀Ni₂₀Cu₄₀P₁₇B₃ metallic glassy ribbons were carried out at a classical three-electrode setup in CHI760D electrochemical workstation. (Pt foil: counter electrode, saturated calomel electrode: reference electrode) in 0.8 mol·L⁻¹ H₂SO₄ + 0.2 mol·L⁻¹ H₃PO₄ solutions. The chemical compositions of the NPMs were characterized by energy dispersive X-ray spectrometer (EDS) and the microstructures were observed by transmission electron microscope (TEM). Using a three-electrode electrochemical cell (NPM catalysts on glassy carbon electrode: working electrode, Pt foil: counter electrode, mercury sulfate electrode: reference electrode) in CHI 760D electrochemical workstation, the electrochemical properties of the NPMs were evaluated by cyclic voltammetry (CV) and chronoamperometry tests in 0.5M H₂SO₄ and 0.5M H₂SO₄ + 0.5M HCOOH solutions.

3. Results and Discussion

In order to determine the proper dealloying potential range, the linear polarization tests were performed on the Pd₂₀Ni₆₀P₁₇B₃ and Pd₂₀Ni₂₀Cu₄₀P₁₇B₃ glassy ribbons in 0.8 mol·L⁻¹ H₂SO₄ + 0.2 mol·L⁻¹ H₃PO₄ solutions. As shown in Figure 1, the polarization curve of the Pd₂₀Ni₆₀P₁₇B₃ glass can be divided into four different steps: Firstly, the glassy ribbons are spontaneously passivated in 0-650 mV. In this potential range, dealloying can hardly take place. Secondly, a

*e-mail: zyuqiao@seu.edu.cn

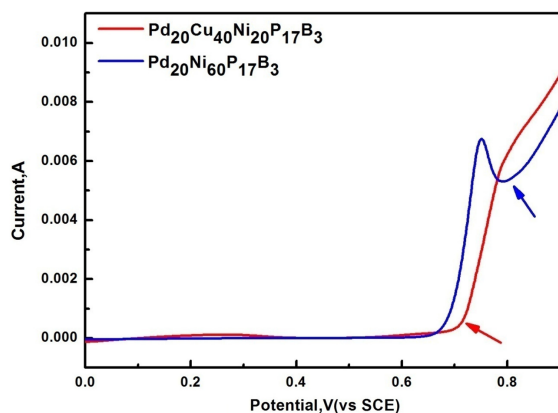


Figure 1. polarization curves of the Pd₂₀Ni₆₀P₁₇B₃ and Pd₂₀Ni₂₀Cu₄₀P₁₇B₃ metallic glasses, measured in 0.8 mol·L⁻¹ H₂SO₄ + 0.2 mol·L⁻¹ H₃PO₄ solutions (vs SCE).

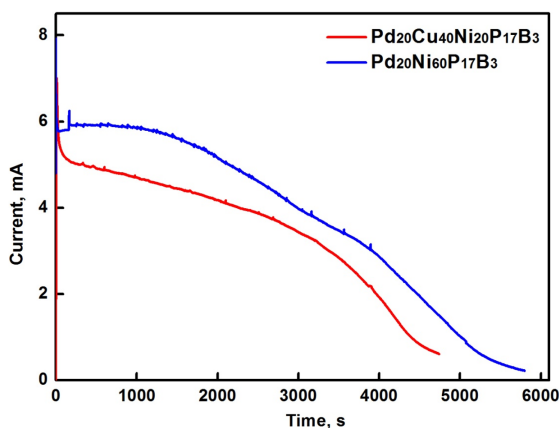


Figure 2. current vs time curves of the Pd₂₀Ni₆₀P₁₇B₃ and Pd₂₀Ni₂₀Cu₄₀P₁₇B₃ metallic glasses in 0.8 mol·L⁻¹ H₂SO₄ + 0.2 mol·L⁻¹ H₃PO₄ solutions.

remarkable current rise appears at about 680 mV and after that the current keeps in a linear relationship with the increasing potential up to 750 mV. A transient passivation-like behavior appears at higher potentials ranging from 750 to 800 mV, followed by a current rise from 820 mV. In order to avoid passivation and form NPM, the applied dealloying potential of the Pd₂₀Ni₆₀P₁₇B₃ is 820 mV at the second apex nasi. In the case of the Pd₂₀Ni₂₀Cu₄₀P₁₇B₃ glass, the polarization curve is simpler, i.e. a large passivation range lies in 0-680 mV, followed by a single apex nasi (critical dealloying potential) where the selective corrosion of Ni, Cu and P from the metallic glass starts¹⁴. After that, the current increases dramatically with the further increase of the applied potential. Therefore, 680 mV was chosen as the applied dealloying potential for the Pd₂₀Ni₂₀Cu₄₀P₁₇B₃ glass. When the Pd₂₀Ni₆₀P₁₇B₃ and Pd₂₀Ni₂₀Cu₄₀P₁₇B₃ metallic glasses are potentiostatically dealloyed at 820 mV and 680 mV, respectively, the corresponding current-time curves are recorded and shown in Figure 2. Similar as that of dealloying crystalline alloys, both of the glassy samples first experience an initial current rising stage. Then after a slight current drop, the dealloying process comes into a slow current decay stage¹⁵. When the dealloying current drops to about 0 mA, the dealloying process is completed. The as-obtained dealloyed samples are named as NPM 1# and NPM 2# when the precursor glassy ribbons are Pd₂₀Ni₆₀P₁₇B₃ and Pd₂₀Ni₂₀Cu₄₀P₁₇B₃, respectively.

The chemical compositions of the NPMs are measured by EDS. Both NPMs contain Pd higher than 80 at%, indicating that Pd-based NPMs are obtained. NPM1# has 82 at% of Pd, 8 at% of Ni, and 10 at% of P. NPM2# has 86 at% of Pd, 3 at% of Ni, and 7 at% of Cu and 4 at% of P. The residuals of a small amount of Ni, Cu and P in NPMs may be related to the core-shell structure^{15,16}. When more positive elements (Ni, Cu, B and P in this research) dissolve, the inert Pd atoms will be liberated and accumulated on the surface of ligaments, forming a Pd or Pd-rich shell. If the applied dealloying potential is higher than the critical dealloying potential of the newly formed shell, more Ni and P will dissolved until an alloy with a higher Pd content or pure Pd shell is formed and no further dissolution is possible.

The TEM diffraction patterns of the dealloyed samples in the insets of Figure 3a, b indicate that the amorphous structure in the precursors has been totally changed into pure face-centered cubic phase after the dealloying process. The lattice parameters deduced from the diffraction results are about 0.388 nm and 0.383 nm for NPM 1# and NPM 2#, respectively, similar to that of the pure fcc Pd (0.389 nm). Figure 3a, b displays the bright-field TEM images of NPM1# and NPM 2#. Both of the samples contain a large number of open, three-dimensional, interpenetrating nanopores. The metallic ligaments are about 20 nm in width, while the pore size is much smaller. Figure 3c, d reveals the distribution ratio of the pore size in NPM 1# and NPM 2#. The characteristic length scales of the pores are about 5.2 nm in NPM 1# and 5.0 nm in NPM 2#, respectively, indicating that NPM 1# and NPM 2# have a similar nanoporous structure.

The electrocatalytic activities of the Pd-based NPMs toward the oxidation of formic acid were characterized by cyclic voltammetry in an acid electrolyte. A commercial Pd/C catalyst is also involved for comparison. The electrochemical active surface area (ECSAs) is estimated from the integration of the reduction peak of Pd. Figure 4a shows the CV curves in 0.5 mol/L H₂SO₄ solution. For the three different catalysts, a peak appears in the region of 0-0.20 V during the positive scanning, which can be attributed to the adsorption and desorption of H⁺¹⁷. The peak around 1.0 V is associated with the oxidation of Pd^{13,18}. It can be seen from the CV curves, that NPM 1# and NPM 2# exhibit a similar desorption and oxidation behavior. Figure 3b displays the CV curves in 0.5 mol/L H₂SO₄ + 0.5 mol/L HCOOH. All the three catalysts show a clear peak at 0.25-0.40 V, corresponding to the oxidation of the formic acid. When compared with the commercial Pd/C (0.40 V), the oxidation potential on the NPMs is much lower, i.e. 0.31 V on NPM 1# and 0.27 V on NPM 2#, indicating that the NPMs obtained in this work have higher catalytic activity than the Pd/C. It should be noticed that though NPM 1# and NPM 2# have similar nanoporous structure, they exhibit different catalytic activity. The reason may be related to the different chemical compositions. Firstly, NPM 2# has higher Pd content than NPM 1#. In the Pd-based

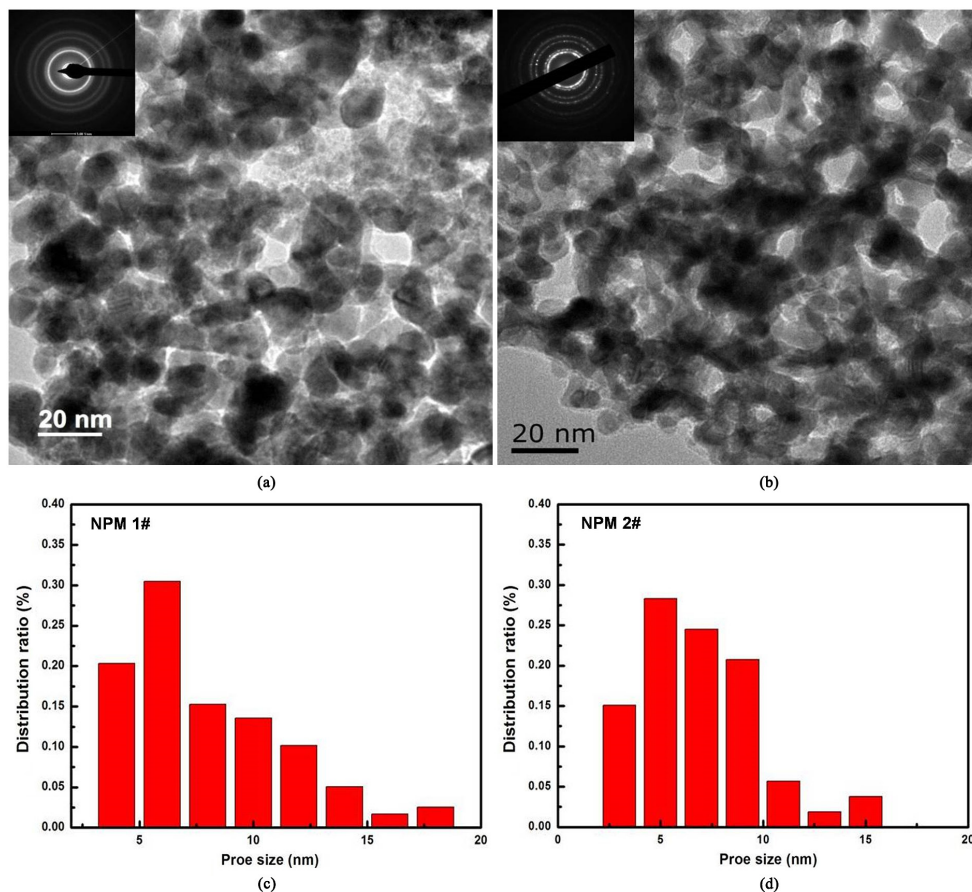


Figure 3. Bright-field TEM images of the NPM 1# (a) and NPM 2# (b), the insets are the SEAD patterns of the corresponding NPMs; the pore size distribution in NPM 1# (c) and NPM 2# (d).

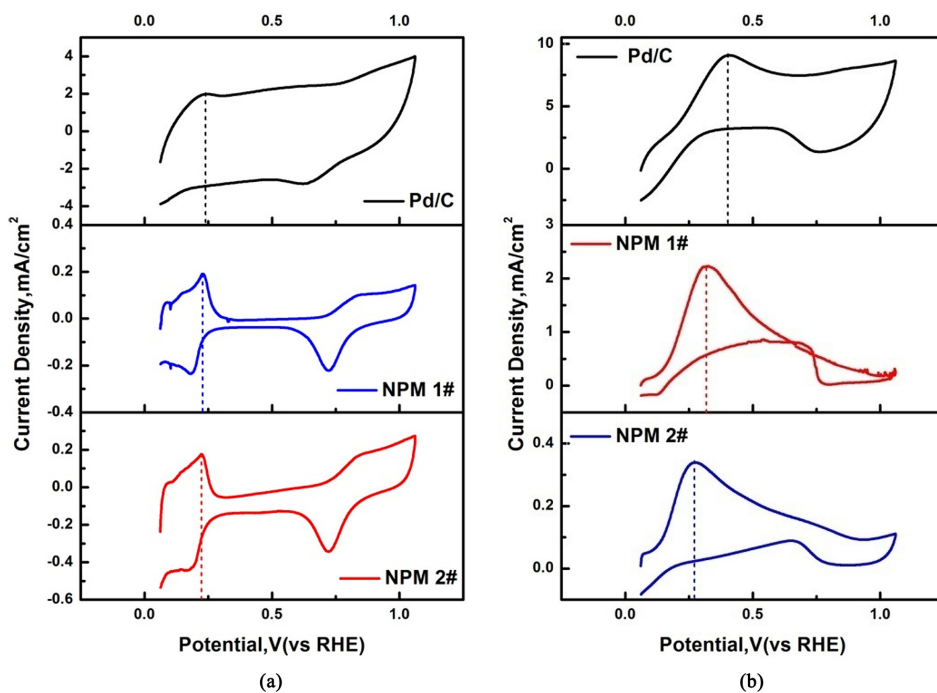


Figure 4. Cyclic voltammograms in 0.5 M H₂SO₄ (a) and in 0.5 M H₂SO₄+0.5 M HCOOH solutions (b) under a scan rate of 50 mV s⁻¹ (vs RHE).

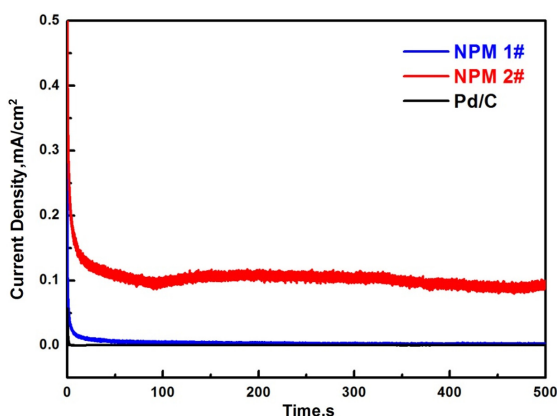


Figure 5. Chronoamperometric current density-time curves in 0.5 M $\text{H}_2\text{SO}_4 + 0.5 \text{ M HCOOH}$ solutions.

NPMs, only the Pd sites are the active sites which will take part into the catalytic reaction. Thus, the higher Pd content will benefit the catalytic activity. Secondly, there are some atoms in NPM 2#. The extra Cu atoms can modify the d bond of Pd and make it easier for Pd to pass their electrons to O_2 during the catalytic process¹⁹⁻²¹. Similar results can also be found in the report of Xu et al.²². In a nanoporous PdCu alloy, the Cu atoms buried under the topmost Pd layer

lower the d-band center of Pd, resulting in more excellent catalytic performance.

The catalytic stability of the NPMs was evaluated by chronoamperometry test in 0.5 mol/L $\text{H}_2\text{SO}_4 + 0.5 \text{ mol/L HCOOH}$ solutions. For comparison, the commercial Pd/C is also involved in the experiment. In Figure 5, it can be found that the NPM 2# shows the highest oxidation current density at 500 s (0.10 mA/cm²), which is about 10 times of the Pd/C and NPM 1#. The addition of Cu into the NPM 2# may contribute to the high stability. It has been well accepted that the decrease of the catalytic activity on NPMs is mainly caused by the structure coarsening. In many NPMs, such as NPd and NPPt, the Cu addition has been proved to play an important role on stabilizing the nanoporous structure. In this study, the Cu addition may take the same effects in NPM 2# and leads to higher catalytic stability.

4. Conclusions

The $\text{Pd}_{20}\text{Ni}_{60}\text{P}_{17}\text{B}_3$ and $\text{Pd}_{20}\text{Ni}_{20}\text{Cu}_{40}\text{P}_{17}\text{B}_3$ metallic glasses were potentiostatically dealloyed in acid solutions. Though the porous structure size of the as-obtained NPMs is similar, the catalytic performances vary according to the different glassy precursors. The NPM prepared by dealloying $\text{Pd}_{20}\text{Ni}_{20}\text{Cu}_{40}\text{P}_{17}\text{B}_3$ shows higher catalytic activity and stability toward the formic acid electrooxidation. The Cu residuals may contribute to the improved catalytic performances.

References

- Winter M and Brodd RJ. What are batteries, fuel cells, and supercapacitors? *Chemical Reviews*. 2004; 104(10):4245-4270. <http://dx.doi.org/10.1021/cr020730k>. PMID:15669155.
- Yan L, Yao SK, Chang JF, Liu CP and Xing W. Pd oxides/hydrous oxides as highly efficient catalyst for formic acid electrooxidation. *Journal of Power Sources*. 2014; 250:128-133. <http://dx.doi.org/10.1016/j.jpowsour.2013.10.085>.
- Du C, Chen M, Wang WG and Yin GP. Nanoporous PdNi Alloy nanowires as highly active catalysts for the electro-oxidation of formic acid. *ACS Applied Materials & Interfaces*. 2011; 3(2):105-109. <http://dx.doi.org/10.1021/am100803d>. PMID:21192691.
- Qiu HJ, Ito Y and Chen MW. Hierarchical nanoporous nickel alloy as three-dimensional electrodes for high-efficiency energy storage. *Scripta Materialia*. 2014; 89:69-72. <http://dx.doi.org/10.1016/j.scriptamat.2014.06.031>.
- Yu JS, Ding Y, Xu CX, Inoue A, Sakurai T and Chen MW. Nanoporous metals by dealloying multicomponent metallic glasses. *Chemistry of Materials*. 2008; 20(14):4548-4550. <http://dx.doi.org/10.1021/cm8009644>.
- Ge XB, Wang RY, Liu PP and Ding Y. Platinum-decorated nanoporous gold leaf for methanol electrooxidation. *Chemistry of Materials*. 2007; 19(24):5827-5829. <http://dx.doi.org/10.1021/cm702335f>.
- Tan XL, Li K, Liu Y, Wu WD, Luo JS and Tang YJ. Effects of the dealloying process on the morphology of nanoporous copper. *Rare Metal Materials and Engineering*. 2010; 39(11):2011-2014.
- Liu H, Liu Y, Lian LX, Yu ZW, Sun WZ and Shi B. Fabrication of bulk nanoporous copper by dealloying of $\text{Cu}_{0.3}\text{Mn}_{0.7}$ alloy. *Rare Metal Materials and Engineering*. 2010; 39(11):2007-2010.
- Su XD, Han F, He L, Liu RG, Huang YL, Hao WC, et al. Surface characteristics of NiTi alloys modified by dealloying at low temperature. *Rare Metal Materials and Engineering*. 2011; 40(8):1446-1449.
- Erlebacher J, Aziz M, Karma A, Dimitrov N and Sieradzki K. Evolution of nanoporosity in dealloying. *Nature*. 2001; 410(6827):450-453. <http://dx.doi.org/10.1038/35068529>. PMID:11260708.
- Forty AJ. Corrosion micro-morphology of noble-metal alloys and depletion gilding. *Nature*. 1979; 282(5739):597-598. <http://dx.doi.org/10.1038/282597a0>.
- Rugolo J, Erlebacher J and Sieradzki K. Length scales in alloy dissolution and measurement of absolute interfacial free energy. *Nature Materials*. 2006; 5(12):946-949. <http://dx.doi.org/10.1038/nmat1780>. PMID:17099702.
- Chen M, Wang ZB, Zhou K and Chu YY. Synthesis of Pd/C catalyst by modified polyol process for formic acid electrooxidation. *Fuel Cells (Weinheim)*. 2010; 10(6):1171-1175. <http://dx.doi.org/10.1002/face.201000046>.
- Wagner K, Brankovic SR, Dimitrov N and Sieradzki K. Dealloying below the critical potential. *Journal of the Electrochemical Society*. 1997; 144(10):3545-3555. <http://dx.doi.org/10.1149/1.1838046>.
- Xu JL, Wang Y and Zhang ZH. Potential and concentration dependent electrochemical dealloying of Al_2Au in sodium chloride solutions. *The Journal of Physical Chemistry C*. 2012; 116(9):5689-5699. <http://dx.doi.org/10.1021/jp210488t>.
- Xu CX, Liu AH, Qiu HJ and Liu YQ. Nanoporous PdCu alloy with enhanced electrocatalytic performance. *Electrochemistry Communications*. 2011; 13(8):766-769. <http://dx.doi.org/10.1016/j.elecom.2011.04.007>.
- Habas SE, Lee H, Radmilovic V, Somorjai GA and Yang P. Shaping binary metal nanocrystals through epitaxially seeded

- growth. *Nature Materials*. 2007; 6(9):692-697. <http://dx.doi.org/10.1038/nmat1957>. PMID:17618289.
18. Feng LG, Yao SK, Zhao X, Yan L, Liu CP and Xing W. Electrocatalytic properties of Pd/C catalyst for formic acid electrooxidation promoted by europium oxide. *Journal of Power Sources*. 2012; 197:38-43. <http://dx.doi.org/10.1016/j.jpowsour.2011.09.030>.
 19. Abel M, Robach Y and Porte L. Stress induced surface structures and reactivity of thin layer Pd/Cu(110) deposits. *Surface Science*. 2002; 498(3):244-256. [http://dx.doi.org/10.1016/S0039-6028\(01\)01753-8](http://dx.doi.org/10.1016/S0039-6028(01)01753-8).
 20. Wang L, Wang Y, Song SQ and Shen PK. Density functional theory study on the mechanism for enhanced activity of PdxNi/C catalysts. *Chinese Journal of Catalysis*. 2009; 30:433-439.
 21. Dai L and Zou SZ. Enhanced formic acid oxidation on Cu-Pd nanoparticles. *Journal of Power Sources*. 2011; 196(22):9369-9372. <http://dx.doi.org/10.1016/j.jpowsour.2011.08.004>.
 22. Xu CX, Liu YQ, Wang JP, Geng HR and Qiu HJ. Nanoporous PdCu alloy for formic acid electro-oxidation. *Journal of Power Sources*. 2012; 199:124-131. <http://dx.doi.org/10.1016/j.jpowsour.2011.10.075>.